

MIT Open Access Articles

Microbial metatranscriptomics in a permanent marine oxygen minimum zone

The MIT Faculty has made this article openly available. **Please share** how this access benefits you. Your story matters.

Citation: Stewart, Frank J., Osvaldo Ulloa, and Edward F. DeLong. "Microbial Metatranscriptomics in a Permanent Marine Oxygen Minimum Zone." *Environmental Microbiology* 14.1 (2012): 23–40.

As Published: <http://dx.doi.org/10.1111/j.1462-2920.2010.02400.x>

Publisher: Society for Applied Microbiology and Blackwell Publishing Ltd

Persistent URL: <http://hdl.handle.net/1721.1/69592>

Version: Author's final manuscript: final author's manuscript post peer review, without publisher's formatting or copy editing

Terms of use: Creative Commons Attribution-Noncommercial-Share Alike 3.0



Title: Microbial metatranscriptomics in a permanent marine oxygen minimum zone

5

10

15

Contributors: Frank J. Stewart¹, Osvaldo Ulloa², and Edward F. DeLong^{*1}

Affiliations and footnotes:

20 * Corresponding author. Mailing address: Division of Biological Engineering &
Department of Civil and Environmental Engineering, Massachusetts Institute of
Technology, Parsons Laboratory 48-427, 15 Vassar Street, Cambridge, MA
02139. Phone: (617) 253-5271. Email: delong@MIT.edu

25 ¹Department of Civil and Environmental Engineering, Massachusetts Institute of
Technology, Parsons Laboratory 48, 15 Vassar Street, Cambridge, MA 02139.

30 ²Departamento de Oceanografía and Centro de Investigación Oceanográfica en el
Pacífico Sur-Oriental, Universidad de Concepción, Casilla 160-C, Concepción,
Chile

Running title: OMZ community gene expression

35

Keywords: nitrification, amoA, anammox, denitrification, nitrate reduction, crenarchaea,
Nitrosopumilus, pyrosequencing

Modifications made to this revised manuscript are highlighted in green

40

SUMMARY

Simultaneous characterization of the taxonomic composition and metabolic gene content and expression in marine oxygen minimum zones (OMZs), has potential to broaden perspectives on the microbial and biogeochemical dynamics in these environments. Here, we present a metatranscriptomic survey of microbial community metabolism in the Eastern Tropical South Pacific OMZ off northern Chile. Community RNA was sampled in late austral autumn from four depths (50, 85, 110, 200 m) extending across the oxycline and into the upper OMZ. Shotgun pyrosequencing of cDNA yielded 180,000 to 550,000 transcript sequences per depth. Based on functional gene representation, transcriptome samples clustered apart from corresponding metagenome samples from the same depth, highlighting the discrepancies between metabolic potential and actual transcription. BLAST-based characterizations of non-ribosomal RNA sequences revealed a dominance of genes involved with both oxidative (nitrification) and reductive (anammox, denitrification) components of the marine nitrogen cycle. Using annotations of protein-coding genes as proxies for taxonomic affiliation, we observed depth-specific changes in gene expression by key functional taxonomic groups. Notably, transcripts most closely matching the genome of the ammonia-oxidizing archaeon *Nitrosopumilus maritimus* dominated the transcriptome in the upper three depths, representing 1 in 5 protein-coding transcripts at 85 m. In contrast, transcripts matching the anammox bacterium *Kuenenia stuttgartiensis* dominated at the core of the OMZ (200 m; 1 in 12 protein-coding transcripts). The distribution of *N. maritimus*-like transcripts paralleled that of transcripts matching ammonia monooxygenase genes, which, despite being represented by both bacterial and archaeal sequences in the community DNA, were dominated (>99%) by archaeal sequences in the RNA, suggesting a substantial role for archaeal nitrification in the upper OMZ. These data, as well as those describing other key OMZ metabolic processes (e.g., sulfur oxidation), highlight gene-specific expression patterns in the context of the entire community transcriptome, as well as identify key functional groups for taxon-specific genomic profiling.

INTRODUCTION

70

Oxygen minimum zones (OMZs) play critical roles in marine community structuring and global biogeochemical cycling. Forming at intermediate depths (~100-1000m) in response to high biological oxygen demand and reduced ventilation, OMZs occur naturally in zones of nutrient-rich upwelling but are also expanding throughout the world's oceans as a result of anthropogenic effects, such as enhanced nutrient runoff and climate change (Diaz and Rosenberg 2009; Stramma et al. 2008). This expansion critically impacts marine ecosystems, as OMZs, in which dissolved O₂ often falls below 10 μM, displace oxygen-respiring macroorganisms (e.g., fish) and create anaerobic, microbially-dominated communities whose members exert important effects on marine nitrogen and carbon cycles (Ulloa and Pantoja, 2009).

75

80

OMZ communities are typified by a low diversity and abundance of pelagic macrofauna but a complex microbial community adapted to life along the oxic-anoxic gradient. Notably, OMZ-associated bacteria and archaea mediate oceanic fixed nitrogen loss to the atmosphere through denitrification and the anaerobic oxidation of ammonia to N₂ (anammox) (Codispoti et al., 2001; Kuypers et al., 2005; Ward et al., 2009). OMZs also play significant roles in greenhouse gas cycling, for example through the release of the potent heat-trapping gas nitrous oxide (N₂O). Recent genetic and biogeochemical evidence also suggests a role for pelagic sulfur cycling in OMZs, mediated in part by the dissimilatory metabolism of sulfur-oxidizing bacteria related to endosymbionts of deep-sea bivalves (Stevens and Ulloa, 2008; Lavik et al., 2009; Walsh et al., 2009; Canfield et al., 2010).

85

90

Studies of the Eastern Tropical South Pacific (ETSP) OMZ off northern Chile and Peru have been critical in identifying the organisms and metabolisms characteristic of life in pelagic low oxygen environments. In the ETSP-OMZ, persistent upwelling of nutrient-rich waters drives high primary production in the photic zone (Daneri et al., 2000). As photosynthetically-derived organic matter sinks, it is respired and degraded by aerobic heterotrophs, drawing

95 oxygen down from >200 μM at the surface to less than 1 μM below the oxycline (~50-100m). Throughout the core of the OMZ (~70-500m), oxygen decreases to nM concentrations, or even to anoxia (Revsbech et al., 2009). Oxygen conditions remain depleted throughout the year, creating one of the largest persistently oxygen-deficient regions in the global ocean.

As oxygen declines, anaerobic metabolism becomes increasingly important, significantly
100 altering nutrient and organic matter profiles relative to aerobic zones. Notably, oxidized nitrogen species dominate as oxidants in dissimilatory respiration by both autotrophs and heterotrophs. Autotrophic bacteria within the Planctomycetes have been described in the ETSP-OMZ as the primary group responsible for anammox, the likely predominant pathway for fixed nitrogen loss in this system (Thamdrup et al., 2006; Hamersley et al., 2007; Galan et al., 2009; Lam et al.,
105 2009). However, heterotrophic denitrification, the oxidation of organic matter via a complete sequential reduction of nitrate (NO_3) to N_2 , also occurs in the ETSP-OMZ (Farias et al., 2009), potentially producing ammonia (via organic matter remineralization) and nitrite (via nitrate reduction) for anammox. Though the range of microorganisms mediating denitrification is not fully described, the multiple steps of this pathway likely involve diverse taxonomic groups.
110 Notably, the dissimilatory reduction of oxidized nitrogen species may involve chemoautotrophic sulfur-oxidizing bacteria. Indeed, genomic analysis of the lineage SUP05, a free-living gammaproteobacterial relative of clam endosymbionts sampled from a North Pacific seasonal OMZ, revealed enzymes necessary for the chemolithotrophic oxidation of reduced sulfur, as well as those for nitrate reduction to nitrous oxide (N_2O), suggesting a mechanistic link between
115 pelagic sulfur cycling and denitrification (Walsh et al., 2009). Symbiont-like 16S rRNA gene sequences have been detected in the ETSP-OMZ, suggesting similar processes at work in this system (Stevens and Ulloa, 2008). Additionally, aerobic ammonia oxidation to nitrite (nitrification) along the oxycline and in the upper OMZ is intrinsically linked to the dissimilatory nitrogen transformations at the OMZ core, potentially serving as a vital source of nitrite for
120 anammox and fueling an influx of fixed carbon to the system (Lam et al., 2007; Molina and Farias, 2009). Genetic evidence shows a complex nitrifier community in the ETSP-OMZ

composed of both bacteria and archaea, though the relative contributions of these two groups to ammonia-oxidation remains unclear (Molina et al., 2007; Molina et al., 2010).

Our knowledge of these diverse OMZ metabolisms is based largely on studies of individual pathways (e.g., denitrification, anammox) or taxonomic groups, or on single-gene surveys of phylogenetic (e.g., 16S rRNA) diversity and functional gene abundance (e.g., nitrite reductase, ammonia monooxygenase). However, we know little of the extent to which specific metabolic processes are represented in the exceedingly diverse pool of genes expressed across a complex microbial community. Community-wide analysis of microbial gene expression in natural communities can help identify unforeseen linkages among metabolic processes (McCarren et al. 2010), as well as inform predictions of the relative synchrony between metabolic transformations and DNA, RNA, and protein abundance in diverse microbial assemblages. Here, we present the first survey of pelagic microbial community gene expression (the metatranscriptome) in an oxygen minimum zone, focusing specifically on the ETSP-OMZ off northern Chile.

High-throughput sequencing of the metatranscriptome has provided an unprecedented overview of gene expression in natural microbial communities, but thus far has been restricted to a handful of aerobic marine environments (Frias-Lopez et al., 2008; Hewson et al., 2009; Poretsky et al., 2009; Shi et al., 2009; Hewson et al., 2010). Here, we use pyrosequencing to analyze the community RNA and DNA from four depths spanning the aerobic photic zone (50 m), the oxic-anoxic transition zone (85, 110 m), and the anoxic OMZ core (200 m) at a site on the continental slope. Using BLAST-based characterizations of protein-coding genes, we characterize dominant patterns in metatranscriptome diversity, transcriptional activity, and sample-relatedness, as well as identify key trends in taxonomic and functional gene representation. These datasets facilitate comparative analysis of bacterioplankton gene expression across diverse oceanic regions, as well as intensive exploration of cryptic, but functionally important, metabolic processes, genes, and organisms specific to low-oxygen marine environments.

150 RESULTS AND DISCUSSION

Chemical profiles

Vertical profiles of oxygen and inorganic nitrogen at the sampling site (Station #3, ~1050 m depth; ~30 km northwest of Iquique, Chile; see map in Figure S1A) resembled those described previously for the ETSP off northern Chile (e.g., Farias et al., 2007; Galan et al., 2009) (Fig. S1B). Oxygen dropped from ~230 μM at the surface to ~100 μM near the base of the photic zone (50 m, mid-oxycline), before falling to ~10 μM at the upper boundary of the OMZ (85 m). Within the OMZ core, oxygen hovered near the level of detection with standard oceanographic oxygen sensors, before gradually increasing again below 500 m. Consistent with prior reports (Farias et al., 2007), nitrite began increasing below the oxycline, reaching a broad maximum (>6 μM) near the core of the OMZ (200 m). Nitrate peaked initially at the base of the oxycline (~15 μM), decreased gradually in the upper OMZ, then began increasing again near the core of the OMZ. Ammonium concentrations were low along the profile, rising to ~0.35 μM in the center of the oxic zone before falling to near the limit of detection within the OMZ.

165

Descriptive statistics of community RNA and DNA

Despite rapid advances in sequencing technology, microbial metatranscriptome studies are still relatively rare, with only a handful of these studies also providing coupled metagenomic samples (Frias-Lopez et al., 2008; Urich et al., 2008; Shi et al., 2009; McCarren et al., 2010). As these methods are increasingly applied to diverse ecosystems, it is important to describe general features of the microbial metatranscriptome. We therefore provide statistics describing gene diversity, gene hit count distributions, and relatedness among samples both to establish a

170

framework for ecosystem-specific questions and to build a general understanding of gene
175 expression in natural microbial communities.

Read statistics

Pyrosequencing (Roche 454 FLX technology) of community RNA and DNA across four
depths generated 1.9 and 1.6 million sequence reads, respectively, with mean lengths of 251 bp
180 and 172 bp (Table 1). Of the RNA reads, 37-61% matched ribosomal RNA sequences and were
excluded from further analysis. Given the relatively high abundance of archaea in the samples
(see below), further depletion of rRNA would likely have been possible if archaea-specific probe
sets were included in the subtractive hybridization protocol used here to deplete rRNA (Stewart
et al. 2010). Of the non-rRNA-encoding reads, roughly two thirds of the DNA reads and one
185 third of the RNA reads matched protein-coding genes (bit score > 50) in the NCBI-nr database,
with similar fractions matching the KEGG database (Table 1). The lower overall percentage of
identifiable reads in the RNA data suggests large numbers of non-protein-coding, non-ribosomal
RNA transcripts; a similar observation was made in a study showing abundant non-coding small
RNAs (smRNA) in bacterioplankton transcriptomes from the subtropical North Pacific (Shi et
190 al., 2009), suggesting a need for characterization of the potentially unique smRNA pool in the
OMZ community.

Protein-coding gene diversity and distributions

The protein-coding gene sets were highly diverse, encompassing a total of 436,410
195 unique nr reference sequences representing 7875 taxonomic identifiers (DNA + RNA combined).
Of the reference sequences, only 0.2% were present in all datasets (Table S1), and only 4.2% of
unique transcripts were detected in the expressed gene pool at all depths. In both the DNA and
RNA datasets, the vast majority (>85%) of reference sequences were represented by fewer than 2
reads (Fig. S2). The proportional abundance of each gene was highly variable within the RNA
200 samples (low evenness; Table 2). Calculated for sequence subsets standardized to a uniform

sample size (n=15,000), evenness was significantly lower across all RNA samples compared to DNA, falling to a minimum (0.06) in the 85 m sample (upper OMZ) before increasing with depth into the anoxic zone (110 and 200m). Low evenness in the metatranscriptome was driven by small numbers of highly expressed genes (Fig. S3). Here, 13 to 30% of all identifiable protein-coding transcripts were represented by the 100 most abundant genes. Indeed, a single gene, encoding an ammonium transporter of the nitrifying crenarchaeote *Nitrosopumilus maritimus*, represented over 8% of the coding transcript pool in one sample (85 m; Fig. S3; Table S5). In contrast, the most abundant genes in the DNA samples never exceeded 0.1% of the total (Table S5). The overabundance of highly expressed genes in metatranscriptomic samples presents an obstacle to obtaining statistically significant sequence coverage of low frequency transcripts.

Shared gene content

Shared gene content was used to assess the relatedness between sample pairs. To calculate pairwise shared gene percentages and avoid bias due to variation in dataset size (i.e., large datasets share more reference sequences in common than smaller datasets), subsets of reads were randomly extracted from each dataset, yielding uniform numbers of unique nr references per dataset (mean: 12,606; stdev = 0.3%; Table S2). On average, in DNA vs. DNA pairwise comparisons, only 14.7% of reference sequences (per dataset) were shared between depths. A comparable percentage (mean: 13.2%) was shared between RNA samples, similar to values reported for metatranscriptome samples from two photic zone depths in the subtropical North Pacific (Stewart et al., 2010). Comparisons of DNA to RNA datasets, however, revealed significantly lower percentages of shared genes (mean: 8.8%; $P < 0.01$, t-test). Clustering using shared gene percentage as a similarity metric, as in Snel et al. (1999), confirmed that each RNA sample was on average more closely related to any other RNA sample than to its corresponding DNA sample from the same depth (Table S2), potentially suggesting similarity in expressed gene content despite high physicochemical heterogeneity across depths. However, deeper sequencing will be required to confirm that the observed discrepancy between metagenome and

metatranscriptome gene content is not biased by detection of only the most abundant expressed genes.

230 To further examine sample relatedness, DNA and RNA datasets were hierarchically clustered based on the distribution of reads matching KEGG gene categories and nr taxonomic identifiers (Fig. 1). These analyses revealed several patterns. First, consistent with the results based on shared gene content percentage, DNA datasets clustered apart from RNA datasets. This partitioning indicates that the content of the expressed functional gene pool, as currently
235 detected at this level of sequencing depth, was distinct from that of the total DNA pool and similar across samples, as demonstrated most clearly at the broadest functional category level (KEGG 2; Fig. 1). This pattern is consistent with a previous observation of metabolic functional similarity across surface water metatranscriptomes from geographically diverse open ocean sites (Hewson et al., 2010). However, this clustering pattern may vary depending on the database
240 used for deriving the similarity metric. Indeed, the correlations between RNA samples weakened at finer levels of the KEGG hierarchy (ko gene level) and when the analysis was based not on functional category but on taxonomic identifier (Fig. 1, bottom), though the separation of DNA and RNA samples was maintained. Second, correlations between samples were higher for DNA samples compared to RNA samples, indicating that variation in functional category
245 distributions across depths was greater in the metatranscriptome than in metagenome (Table 2). However, this pattern was violated for the 200 m RNA sample, which more closely resembled the DNA samples in three of the four clustering analyses. This grouping may reflect the transition to the unique microbial community at the core of the OMZ. For example, if the 200 m community was sufficiently distinct from that of the upper depths, the 200 m RNA sample may
250 be recruited into the DNA cluster based on similarity to its corresponding DNA sample. Finally, the DNA samples showed clear vertical clustering, with the upper samples (50 and 85 m) clustering separately from those of the middle OMZ (110 and 200 m). This pattern suggests depth-specific transitions in community structure, with a distinction between oxycline-associated communities and those from the lower, more oxygen depleted depths. However, the consistent,

255 independent clustering of DNA and RNA samples suggests that the functional distinction
between coupled metagenome and metatranscriptome samples is greater than that among
samples from different depths. Deeper sequencing is required to determine whether this pattern
holds as more of the metatranscriptome becomes characterized.

260 *Transcriptional activity*

The transcriptional activity of protein-coding genes varied marginally with depth in the
OMZ. Mean expression ratios (RNA/DNA) calculated across the full datasets showed a spike
just below the oxycline (85 m; Fig. 2). However, this pattern was driven primarily, but not
exclusively, by variation in sample size (total number of protein-coding genes per dataset). At
265 shallower sequencing depths (as in the 85 m RNA sample; Table 1), highly expressed genes
occupy a greater proportion of the total number of unique genes detected; as sampling depth
increases, low frequency genes occupy a greater proportion of the total and thereby depress the
mean expression ratio. After standardizing the datasets to a common size (n=15,000 protein-
coding reads), the increase in expression at 85 m decreased substantially, but remained elevated
270 relative to values in the oxycline and at the OMZ core. It is unclear to what extent transcript
abundance serves as a proxy for cellular activity, particularly given the asynchrony frequently
observed between transcript and protein levels (e.g., Taniguchi et al., 2010). However, prior
reports show that bacterioplankton cell counts reach a secondary local maximum below the
oxycline in the OMZ off Iquique (Molina et al., 2005; Galan et al., 2009), potentially supporting
275 a local increase in metabolic activity in this zone.

Taxonomic diversity

Protein-coding gene sequences

280 The taxonomic identifications of protein-coding genes provide an alternative to ribosomal
RNA-based classifications of taxonomy (e.g., Urich et al., 2008). Here, we present results

characterized by searches against the extensive NCBI-nr database of protein-coding genes. Searches against nr maximized our chances of identifying functional gene diversity, as well as helped identify close relatives whose annotated genomes might be used to inform more targeted analyses of gene expression dynamics at the genome level. Though the relatively short sequences (~200 bp) obtained via FLX-based pyrosequencing do not lend themselves to comprehensive phylogenetic reconstructions, the annotations of nr functional genes matching these sequences (top BLASTX hit) can be used as an approximate taxonomic classification for each read. Here, nr functional gene annotations revealed depth-specific transitions in microbial community composition and transcription across the OMZ. At all depths, the rank abundances of dominant taxa differed between the DNA and RNA pools (Fig. 3,4). Assuming the ratio of RNA to DNA abundance of specific genes reflects the relative metabolic activity level, the data suggest several broad trends, supported in part by the high frequency of reads matching several prominent individual taxa (Fig. 5, Table S3,S4).

First, metabolic activity along the oxic-suboxic transition zone was dominated by Crenarchaea. Up to one third of all identifiable protein-coding transcripts from the upper OMZ and within the oxycline matched a crenarchaeote, including numerous uncultured representatives, as well as two ammonia-oxidizing species for which genome data are available: *Cenarchaeum symbiosum*, a marine sponge symbiont (Preston et al., 1996; Hallam et al., 2006b), and *Nitrosopumilus maritimus* (Nm), a cultured nitrifier isolated from a marine aquarium (Konneke et al., 2005; Schleper et al., 2005). In contrast to other well represented taxonomic groups (e.g., *Pelagibacter*), the proportional representation of crenarchaea was consistently higher in the RNA reads, relative to the DNA, suggesting an active crenarchaeal community at these depths (Fig. 4).

Crenarchaeal genes most highly similar to *Nitrosopumilus maritimus* (Nm) dominated these samples, constituting up to 20% of identifiable transcripts (85 m sample) and exhibiting a mean expression ratio 4.5-fold higher than that of the most abundant taxon represented in the DNA (*Pelagibacter*; Fig. 3-4,S4). Of the protein-coding genes in the Nm genome (n=1795;

Walker et al., 2010), 74%, 81%, and 56% were recovered as top hits in BLASTX searches of the
310 50, 85, and 110 m DNA reads, respectively, with relatively uniform coverage across the genome
(Fig. 5). A smaller proportion of Nm genes (15-41%) was represented in the transcript pool,
likely reflecting (in part) the smaller size of the RNA datasets (Table 1).

These results support prior studies underscoring the ubiquity of crenarchaeal-like
Archaea in the global ocean. Hallam et al. (2006) reported a high percentage of DNA sequences
315 closely matching the genome of the crenarchaeal nitrifier *Cenarchaeum symbiosum* (mean 65%
amino acid identity) during winter in the Sargasso sea. A more recent analysis of the suboxic
zone of the Black Sea revealed that up to one quarter of all prokaryotic cells fell within a single
clade of nitrifying crenarchaea closely related to Nm (Labrenz et al., 2010). Walker et al. (2010)
recently reported that an average of 1.2% of the sequences present in the Global Ocean Sampling
320 (GOS) database match Nm across diverse physiochemical habitats and geographic locations. In
their analysis, the majority of DNA reads mapping to Nm shared > 50% amino acid identity with
the reference genome. In our study, reads matched Nm at high identity (mean: 74-75% for
DNA, 70-81% for RNA across depths), with the majority of top Nm hits > 75% identical to the
reference (median: 76-78% for DNA, 64%-84% for RNA). Consistent with previous studies
325 (Hallam et al., 2006b; Walker et al., 2010), our analysis identified several gaps in genome
coverage, perhaps highlighting regions unique to the cultured strain (Fig. 5). Our data, along
with supporting studies, highlight an emerging perspective of crenarchaeal dominance in the
pelagic nitrification zone separating oxic from suboxic waters.

Second, protein-coding gene annotations confirm a prominent sulfur-oxidizing microbial
330 community in the ETSP-OMZ. DNA and RNA reads from the OMZ core were particularly
enriched in sequences matching the genomes of sulfur-oxidizing endosymbionts
(gammaproteobacteria) of deep-sea clams (*Candidatus* *Ruthia magnifica* (Rm) and *Candidatus*
Vesicomysocius okutanii (Vo); Kuwahara et al., 2007; Newton et al., 2007) and the symbiont-
like SUP05 lineage isolated from a seasonally anoxic fjord off British Columbia (Walsh et al.,

335 2009) (Fig. 3). At all depths, the proportional abundance of these taxa was greater in the DNA
than in the RNA, indicating reduced transcriptional activity relative to other groups (e.g.,
crenarchaea; Fig. 4). These results are consistent with prior genetic and genomic surveys.
Indeed, ribosomal RNA gene (16S) sequences related to those from sulfur-oxidizing Rm and Vo
endosymbionts have been recovered from diverse low oxygen regions including the ETSP
340 (Stevens and Ulloa, 2008), the coastal North Pacific (Zaikova et al., 2010), the Arabian Sea
(Fuchs et al., 2005), and the upwelling zone off Namibia (Lavik et al., 2009). Furthermore, the
metagenome of the SUP05 lineage has been sequenced (Walsh et al. 2009), revealing genes
required for sulfur oxidation, carbon fixation, and nitrate reduction. This metabolically versatile
bacterium is hypothesized to oxidize reduced sulfur via the dissimilatory sulfite reductase (DSR)
345 and sox pathways, using nitrate as a terminal electron acceptor (Walsh et al. 2009). Here, our
reads matched a diverse SUP05 gene set at relatively uniform abundance, with 73% of the genes
encoded in the SUP05 metagenome detected in the 200 m DNA sample (Fig. 5). Together, these
studies confirm that organisms capable of chemolithotrophic oxidation of sulfide, likely with
nitrate (Walsh et al. 2010; Lavik et al. 2009), are a common component of pelagic low oxygen
350 environments.

Third, bacteria capable of anaerobic ammonia oxidation (anammox) are common and
transcriptionally active at the core of the OMZ. Notably, reads matching the anammox
planctomycete *Candidatus* Kuenenia stuttgartiensis (Ks) increased with depth to 7.9% of total nr
hits in the 200 m RNA sample, 1.7-fold higher than the proportional representation of Ks in the
355 corresponding DNA (Fig. 3). RNA reads matched a total of 705 distinct Ks genes (out of a
possible 4681; (Strous et al., 2006), with a mean expression ratio of 9.3 per gene, comparable to
that recorded for Nm at the oxycline (6.8) and considerably higher than that for SUP05 at the
same depth (2.6; Fig. 5). Prior ribosomal RNA gene surveys indicate that the majority of OMZ-
associated planctomyces actually cluster within the marine *Candidatus* Scalindua group

360 (Kuypers et al., 2003; Woebken et al., 2008; Galan et al., 2009), rather than with Ks, which was characterized from a wastewater-fed laboratory bioreactor (Strous et al., 2006). This clustering is consistent with the relatively low mean amino acid identity observed here for reads matching Ks (64%; Fig. 3,5), likely reflecting the scarcity of planctomycete genome data (e.g., *Scalindua* spp. protein-coding genes) in the NCBI-nr database.

365 Finally, several taxa were consistently abundant throughout the OMZ but contributed disproportionately to the total transcript pool. For example, the ubiquitous marine alphaproteobacterial genus *Pelagibacter* dominated the DNA at all depths (15% to 22% of all identifiable protein-coding genes; Fig. 3), consistent with prior reports based on 16S clone libraries (Stevens and Ulloa, 2008). DNA reads matching a single genotype, *Pelagibacter* sp. HTCC7211 from the oligotrophic Sargasso Sea (Carlson et al., 2009), reached 12% of the total in the 50 and 85 m samples, and covered 89% of the protein-coding genes in the reference genome (Fig. 5). However, the mean expression ratio for HTCC7211 genes in this sample was relatively low (1.5, compared to a sample mean of 2.0) and all *Pelagibacter* species were consistently underrepresented in the RNA pool (Fig. 1,4,S4). This trend emphasizes the potential disconnect
375 between genomic abundance and metabolic activity.

Ribosomal RNA gene sequences

DNA reads matching ribosomal RNA gene sequences constituted a small fraction of the total reads (16S rRNA reads <1%), but nonetheless provided a broad overview of the relative
380 abundance of major taxonomic groups (Fig. S5). At a general level, patterns in 16S reads paralleled those of the protein-coding DNA pool. Notably, alphaproteobacteria sequences were consistently abundant throughout the OMZ (~1/3 of 16S reads at all depths), reflecting the strong representation of *Pelagibacter* species in the non-rRNA reads. Gammaproteobacteria were equally well-represented, though slightly less abundant than reported previously for the OMZ off Iquique (Stevens and Ulloa, 2008). Consistent with a spike in non-rRNA genes matching
385 *Candidatus* *Kuenenia stuttgartiensis*, planctomycete 16S reads peaked at the core of the OMZ

(200 m). Archaea represented less than 15% of 16S sequences at all depths, with crenarchaeal sequences constituting ~5% of 16S reads in the upper OMZ and above the oxycline, then declining in abundance into the suboxic depths. This pattern parallels the gradient in protein-coding DNA but belies the disproportionately strong expression signal from the crenarchaeal community. A similarly asynchronous signal has been observed in the central Pacific Ocean, where the relative abundance of crenarchaeal ammonia monooxygenase (*amoA*) gene sequences was disproportionately low relative to *amoA* transcript abundance (Church et al., 2010). Such patterns highlight the potential of numerically non-dominant members of the community to contribute significantly to microbial community metabolic activity.

Functional trends

Reads matching NCBI-nr functional genes and KEGG categories provide an overview of the functional processes driving transcriptional activity in the OMZ (see also Fig. S6-S11, Table S5-S8). Exhaustive characterization of the functional genes and pathways represented in our data is beyond the scope of a single analysis. However, several dominant trends emerge from our survey and are highlighted here.

405 *Ammonia oxidation*

Transcript distributions underscore a prominent role for crenarchaeal nitrification along the oxic-suboxic transition zone. Crenarchaeal *amo* sequences, encoding the subunits of ammonia monooxygenase (AmoABC) were among the most highly expressed genes in the 50, 85, and 110 m samples, representing 2.7-4.7% of all sequences identified by KEGG searches, exhibiting expression ratios of 85-167 (Table S5, Fig. S8). In contrast to prior studies suggesting a role for bacterial nitrifiers in the Chilean OMZ (Molina et al., 2007; Lam et al., 2009), as well as to our DNA results which show a mixture of both bacterial and archaeal *amo* genes in the OMZ metagenome, the expressed *amo* transcripts were dominated exclusively by crenarchaeal

sequences (98-100%; Fig. S9). These data corroborate recent results showing the relative
415 dominance of archaeal *amoA* gene sequences in clone libraries and Q-PCR assays from
permanent OMZ sites off Chile and Peru (Molina et al., 2010). Here, transcripts matching Nm
amo genes were particularly well-represented (Table S5). While Nm has been shown
experimentally to oxidize ammonia to nitrite, Nm *amo* genes have relatively low similarity to
characterized bacterial *amo* genes and may encode a unique functional variant of the enzyme;
420 indeed, other genes involved in nitrification (e.g., hydroxylamine oxidoreductase) are lacking
from this organism (Konneke et al., 2005; Hallam et al., 2006b; Hallam et al., 2006a; Walker et
al., 2010). Together, our results confirm a major role for crenararchaeal ammonia-oxidation
along the oxycline and into the OMZ, consistent with a growing body of literature describing the
ubiquity and potential dominance of archaeal nitrification in diverse marine habitats (see
425 (Wuchter et al., 2006), and references in (Prosser and Nicol, 2008; Erguder et al., 2009).

Ammonium transport

Membrane transport processes predominated in the OMZ metatranscriptome (Fig. S6-8),
corroborating prior reports showing the general importance of transport functions in marine
430 bacterioplankton across diverse environments (Frias-Lopez et al., 2008; Sowell et al., 2009;
Poretsky et al., 2010). While transcripts encoding ATP-dependent ABC transporters were
consistently abundant throughout the OMZ (5-6% of total KEGG hits; Fig. S7), those encoding
proton motive force-dependent nitrate transporters (e.g., NarK) increased markedly with depth,
paralleling a similar increase in nitrate reductase transcription (see below). In contrast, other ion
435 coupled transporters peaked at the oxycline and in the upper OMZ (Fig. S7-8), before declining
markedly toward the OMZ core. Notably, transcripts encoding an ammonium transporter (Amt)
constituted 11% of all reads with matches in the nr-database and 18.4% of all reads matching the
KEGG database in the 85 m sample (Table S5, Fig. S8-9). Of the Amt-like reads identified at
this depth, 93% matched genes belonging to crenarchaea, with the ammonium transporter of *N.*
440 *maritimus* (accession ABX13594) representing the single most abundant reference gene across

all datasets (Table S5). In contrast, crenarchaea represented only 16% of the Amt-like reads in the DNA pool at this depth, emphasizing the sometimes striking differentiation between gene (or taxonomic) representation and functional expression (Fig. S9).

The mechanistic basis for high Amt expression in the crenarchaeal community is unclear.

445 It is tempting to speculate that active ammonium transport is required to support nitrification (Hallam et al., 2006b; Hallam et al., 2006a). Indeed, ammonium accumulation via active transport has been shown for nitrifying bacteria (*Nitrosomonas*), and suggested as a mechanism for meeting internal kinetic requirements for ammonia oxidation when environmental concentrations and passive ammonia diffusion rates are low, as is common in marine
450 environments (Schmidt et al., 2004; Weidinger et al., 2007). However, less is known about Amt function in archaea (Andrade and Einsle, 2007; Leigh and Dodsworth, 2007), and the relative contributions of Amt-based transport to energy metabolism and biosynthesis have not been explored. Interestingly, recent experiments on cultured cells show that *Nitrosopumilus maritimus* has a remarkably high affinity for reduced nitrogen, among the highest ever recorded
455 for microbial substrates (Martens-Habbena et al., 2009). This affinity is hypothesized to allow Nm to effectively compete against bacterial nitrifiers, as well as against other marine phototrophs and heterotrophs for ammonium in ammonium-depleted waters. In the ETSP-OMZ, *amt* transcripts paralleled *amo* transcripts in Nm-like crenarchaea, raising the hypothesis that the unprecedented capacity for ammonium acquisition in cultured ammonia-oxidizing crenarchaea
460 may be linked to overexpression of ammonium transporters. However, the extent to which this hypothesis applies to *in situ* conditions in the OMZ is uncertain, as OMZ crenarchaea thrive along the oxycline where ammonium is available and produced at high rates (Fig. S1) (Molina et al., 2010).

465 *Anaerobic nitrogen metabolism*

RNA profiles confirmed a significant transition to anaerobic nitrogen metabolism with depth in the OMZ. Genes encoding the multi-subunit dissimilatory nitrate reductase (*nar*), present in both the traditional denitrification pathway and in anammox, were detected at all depths but were proportionately most abundant in the RNA samples (relative to DNA) and at the core of the OMZ (Table S5, Fig. S10). Specifically, *narG*, encoding the alpha subunit of the enzyme, increased with depth to represent 1% of all identifiable protein-coding genes in the 200 m transcriptome. The pattern of *narG* sequence diversity differed substantially between the DNA and RNA pools (Fig. S10). Diverse *narG* sequences were detected at all depths in the DNA, representing between 32 and 389 distinct nr reference genes and suggesting a range of taxa with the capacity for nitrate respiration. In contrast, the *narG* transcript pool was strikingly uniform in the upper OMZ, where all transcripts from the 50 m and 85 m samples matched a single reference sequence, from the anammox planctomycete *Candidatus* *Kuenenia stuttgartiensis* (Ks; Fig. S10). In contrast, at 200 m the nitrate reductase transcript pool was incredibly diverse, representing 187 distinct nr reference sequences from diverse taxa, including the symbiont-like sulfur oxidizers Vo and SUP05. This transition in transcript diversity highlights a community-wide shift to nitrate as a terminal electron acceptor at the OMZ core (or anammox end product; Strous et al., 2006), emblematic of the high potential denitrifier diversity in OMZs (Castro-Gonzalez et al., 2005; Jayakumar et al., 2009).

A strong representation of key planctomycete functional genes suggests a prominent role for anammox in the OMZ. Notably, the proportional abundance of transcripts encoding planctomycete hydrazine/ hydroxylamine oxidoreductase (HAO), an enzyme critical to the conversion of hydrazine to N₂ during anammox (Kuenen, 2008), increased 300-fold from the 50 m to the 200 m sample, accounting for a maximum of 1.4% of all identifiable protein-coding reads (NCBI-nr matches, summed across multiple taxa). Of these reads, 98% matched sequences annotated as planctomycetes. Planctomycete *narG* sequences, predominantly those matching Ks (see above), were also well represented, but were proportionately most abundant when planctomycete HAO transcripts were rare (Fig. S10). The molecular basis of the anammox

reaction is not completely understood, but likely involves the Nar enzyme acting in reverse to oxidize nitrite to nitrate, pumping electrons into transport systems to fuel autotrophy (Strous et al., 2006; Jetten et al., 2009). However, anammox bacteria may also use Nar to oxidize organic matter with nitrate. Indeed, anammox planctomycetes are much more metabolically diverse than previously thought and have been shown to use organic acids as electron donors to reduce nitrate and nitrite and to out-compete heterotrophic denitrifiers for these substrates (Kartal et al., 2007a; Kartal et al., 2007b; Kartal et al., 2008).

500

Sulfur energy metabolism

Transcripts from diverse pathways confirm the activity of sulfur-based energy metabolism in the OMZ (Table S6). Notably, genes of the dissimilatory sulfite reductase enzyme (Dsr), the sulfur oxidation (Sox) gene complex mediating thiosulfate oxidation, and the adenosine 5'-phosphosulfate (APS) reductase (Apr) were expressed throughout the OMZ (Table S6-8), with the greatest proportional representation coming from *dsr* genes at the OMZ core. Several of the proteins encoded by these genes, including Dsr and Apr enzymes, function in both oxidative and reductive pathways. Notably, homologs encoding AprBA and DsrAB are present in a wide range of chemolithotrophic sulfur-oxidizers, as well as sulfate-reducers (Dhillon et al., 2005; Meyer and Kuever, 2007b, a). These genes share ancestry and structure but can be differentiated into distinct phylogenetic clades. Here, the majority (>90%) of *aprAB* and *dsrAB* transcripts matched genes in NCBI-nr belonging to sulfur-oxidizing organisms, including green and purple sulfur bacteria, the SUP05 lineage, and thiotrophic symbionts of diverse hydrothermal vent and seep fauna (Table S7-8). The detection of transcripts encoding the nitrate reductase present in several of these taxa (e.g., SUP05 and the symbiont *Candidatus Vesicomysocius okutanii*; Fig. S10) suggests dissimilatory sulfur oxidation with nitrate in the OMZ and therefore a potential coupling between sulfur oxidation and denitrification in the OMZ. Indeed, recent

520 experimental analyses of water from below the oxycline in the Chilean OMZ demonstrates a
direct coupling between sulfide oxidation and nitrate reduction to both nitrite and nitrous oxide
(Canfield et al., 2010), consistent with prior suggestions of coupling between marine sulfur and
nitrogen cycles in other redox-stratified zones (Jensen et al., 2009; Lavik et al., 2009). In
conjunction with these studies, our data indicate an active sulfur cycle in the OMZ, highlighting
the need for experimental metatranscriptomic analyses (e.g., bioreactor experiments) in which
community sulfur (and nitrogen) metabolism can be directly monitored relative to biochemical
525 rate measurements and in response to environmental perturbations.

These results highlight only a small subset of the exceedingly diverse network of genes
expressed in the OMZ. Indeed, further examination of these datasets is warranted, and many
interesting trends present in the data will emerge as more complementary data sets accumulate.
530 For example, the relative abundance of transcripts encoding transposases increased 23-fold from
the 50 m to the 200 m sample, paralleling a similar increase in the genomic DNA (Fig. S11).
Overrepresentation of transposases with depth in DNA has been reported for bacterioplankton in
the North Pacific Subtropical Gyre, where transposase abundance in metagenomic libraries
increased ~30-fold from the surface to 4000 m (Delong et al., 2006; Konstantinidis et al., 2009).
535 This trend was shown to parallel a general decrease in purifying selection pressure with depth,
leading the authors to hypothesize a causal relationship between relaxed selection and mobile
element expansion (Konstantinidis et al., 2009). Though the ultimate factor(s) driving this
pattern remain unclear, our data support a global trend in depth-specific mobile element activity
that spans both oxic and suboxic conditions. In this coastal OMZ environment, the gradient of
540 mobile element expansion versus depth appears much steeper than in the open ocean. Additional

comparative analyses of individual genes and pathways will likely reveal other globally conserved processes operating in the OMZ

Conclusions

545

A central challenge in environmental microbiology is to place individual genes and species in the context of the integrated communities in which they operate. High-throughput sequencing of community RNA takes an important step in this direction, providing snapshots in time of the proportional abundance of tens of thousands of diverse transcripts. Here, we present the first survey of an OMZ metatranscriptome, with two broad goals.

550

First, at a general level, we characterized the sequence diversity and relatedness between coupled metagenomic and metatranscriptomics datasets using descriptive statistics (e.g., evenness) and clustering. Though metatranscriptomic analyzes are being increasingly applied to natural microbial communities, only a small number of studies have analyzed both DNA and RNA sequence pools in tandem (Frias-Lopez et al. 2008; Urich et al., 2008; Shi et al., 2009). The extent to which current sequencing and analytical methods capture the diversity in these two pools remains poorly described. Here, despite read counts in the hundreds of thousands, minimal overlap in individual gene content occurred between datasets, although clustering based on broader functional gene categories identified similarity in expressed gene content across samples. The latter may be consistent with a broader trend in functional conservation in the highly expressed gene set (e.g., Hewson et al., 2010), but confirmation of this pattern requires comparative analysis of diverse microbial metatranscriptomes, which so far have been characterized primarily for marine bacterioplankton. In conjunction with prior studies, our results describe the marine microbial metatranscriptome as dominated by small numbers of highly expressed genes (e.g., *amt* genes in this study, as in Frias-Lopez et al., 2008 and Hewson et al. 2010), emphasizing a need for greater sequencing depth to adequately characterize low

560

565

frequency transcripts, as well as potential functional (or evolutionary) differences among genes with varying expression patterns. Targeted removal of highly expressed protein-coding genes, potentially via modification of existing subtractive hybridization protocols (e.g., Stewart et al., 2010), may enable more comprehensive characterizations of functional diversity in the microbial metatranscriptome.

Secondly, these datasets provided a snapshot of dominant taxonomic and functional trends in the Chilean OMZ at the time of collection. This analysis was simplified in part by focusing on sequences matching specific organisms diagnostic of key OMZ functions (e.g., nitrate reduction, anammox, sulfur oxidation), an approach facilitated by comparisons against the extensive NCBI-nr database. Notably, these data identify nitrification by crenarchaeal relatives of *Nitrosopumilus maritimus* as a dominant energy source in the upper OMZ (in late autumn 2008), suggesting this group as a candidate for more intensive taxon-specific genomic analyses over temporal gradients. Additionally, together with other recent analyses (Lavik et al., 2009; Walsh et al., 2009; Canfield et al., 2010), our results indicate the presence of an active sulfur oxidizing community in the Chilean OMZ, showing the expression of a diverse set of dissimilatory sulfur oxidation genes and identifying a South Pacific relative of the SUP05 lineage as a dominant and active component of the OMZ community with potential direct ties to the denitrification pathway. However, dominant trends were highlighted here at the expense of more cryptic, but potentially equally important, patterns that could not be adequately addressed in a single study (e.g., carbon-fixation pathways). These datasets therefore provide a reference point for more targeted follow-up studies of specific pathways, ideally involving hypotheses that can be tested through direct experimentation or corroborated by metabolic rate measurements. As more metatranscriptome datasets become available, the integration of these and other data will facilitate comparative studies exploring fundamental features of microbial gene expression that occur across dynamic redox gradients.

595 **EXPERIMENTAL PROCEDURES**

Sample Collection

Microbial community DNA and RNA samples were collected from the ETSP OMZ as part of the Microbial Oceanography of Oxygen Minimum Zones (MOOMZ-1) cruise aboard the
600 *R/V Vidal Gormaz* (June 12-23, 2008). Seawater was sampled from four depths (50 m, 85 m, 110 m, 200 m) at Station #3 (20° 07'S, 70° 23'W; ~1050 m water depth; Fig. S1A) off the coast of Iquique, Chile on June 16-17 using 10L Niskin bottles deployed on a rosette system containing a conductivity-temperature-depth (CTD) profiler (Seabird 25; Seabird Electronics) equipped with an Optode dissolved oxygen sensor. Replicate seawater samples for RNA
605 extraction (n=4 replicates; 1.5-3.0 L seawater per replicate) were pre-filtered through 1.6 µm GF/A filters (47 mm dia., Whatman) and collected onto 0.22 µm Durapore filters (25 mm dia., Millipore) using a peristaltic pump (1.5-3.0 L seawater per filter). Filters were immediately transferred to microcentrifuge tubes containing 300 µl RNeasy Lysis Buffer (Ambion) and frozen at -80°C, with less than 15 min elapsing between sample collection (arrival on deck) and fixation in
610 RNeasy Lysis Buffer. Samples for DNA extraction were collected from the same water sample used for RNA collection, as in Frias-Lopez et al. (2008). For each sample, seawater (15-30 L) was filtered through a 1.6 µm GF/A prefilter (125 mm dia., Whatman) and then collected on a 0.22 µm Steripak-GP20 filter (Millipore). The filter units were filled with lysis buffer (50 mM Tris•HCl, 40 mM EDTA, and 0.75 M sucrose), capped, and frozen at -80°C until extraction.

615

RNA and DNA isolation

Total RNA was extracted from filters using a modification of the *mirVana*TM miRNA Isolation kit (Ambion) as described previously (Shi et al., 2009; Stewart et al., 2010). Briefly,

620 samples were thawed on ice, and the RNAlater® surrounding each filter was removed and discarded. Filters were immersed in Lysis/Binding buffer (Ambion) and vortexed to lyse attached cells. Total RNA was then extracted from the lysate according to the manufacturer's protocol, incubated (37°C for 30 min) with TURBO DNA-free™ to remove genomic DNA, and purified and concentrated using the RNeasy MinElute Cleanup kit (Qiagen). Genomic DNA was extracted from Steripak filters as described previously (Frias-Lopez et al., 2008).

625

rRNA subtraction, RNA amplification and cDNA synthesis

The proportion of bacterial ribosomal RNA transcripts (16S and 23S molecules) in total RNA extracts was reduced via a subtractive hybridization protocol using sample-specific rRNA probes, as described in Stewart et al. [2010]. rRNA-depleted total RNA (~35-100 ng) was then amplified using the MessageAmp™ II-Bacteria kit (Ambion) as described previously (Frias-Lopez et al., 2008; Shi et al., 2009). Briefly, total RNA was polyadenylated using *Escherichia coli* poly(A) polymerase. Polyadenylated RNA was converted to double-stranded cDNA via reverse transcription primed with an oligo(dT) primer containing a promoter sequence for T7 RNA polymerase and a recognition site for the restriction enzyme BpmI (T7-BpmI-(dT)₁₆VN, 635 Table 1). cDNA was then transcribed *in vitro* at 37°C (12-14 hr), yielding large quantities (20-110 µg) of single-stranded antisense RNA. Amplified RNA (~5-10 µg aliquot) was then converted to double-stranded cDNA using the SuperScript® III First-Strand Synthesis System (Invitrogen) with priming via random hexamers for first-strand synthesis, and the SuperScript™ Double-Stranded cDNA synthesis kit (Invitrogen) for second-strand synthesis. cDNA was then 640 purified with the QIAquick PCR purification kit (Qiagen), digested with BpmI for 2-3 hrs at 37°C to remove poly(A) tails, and used directly for pyrosequencing

Pyrosequencing

Poly(A)-removed cDNA was purified for sequencing via the AMPure® kit (Agencourt®) and used for the generation of single-stranded DNA libraries and emulsion PCR according to established protocols (454 Life Sciences, Roche). Clonally amplified library fragments were sequenced with full plate runs on a Roche Genome Sequencer FLX instrument (excluding the 85 m cDNA sample, which was sequenced on a half plate).

650 *Data analysis*

Sequences sharing 100% nucleotide similarity and length (replicates) may represent artifacts generated by preparing samples for pyrosequencing (Gomez-Alvarez et al., 2009; Stewart et al., 2010). Replicates were identified among non-rRNA sequences using the open-source program CD-HIT (Li and Godzik, 2006) and removed from each dataset. Non-replicate reads matching ribosomal RNA genes were identified in cDNA and DNA datasets by BLASTN comparisons to a database containing prokaryotic and eukaryotic small and large subunit rRNA nucleotide sequences (5S, 16S, 18S, 23S and 28S rRNA) compiled from microbial genomes and sequences in the ARB SILVA LSU and SSU databases (<http://www.arb-silva.de>). Reads aligning with bit scores > 50 were identified as rRNA sequences and removed. Small subunit ribosomal RNA reads (16S) from the DNA-based datasets were characterized according to the NCBI taxonomy based on alignments obtained through the greengenes workbench (greengenes.lbl.gov: Fig. S5).

Non-replicate, non-rRNA sequences were characterized by homology searches (BLASTX) against the National Center for Biotechnology Information non-redundant protein database (NCBI-nr, as of Nov. 26, 2009) and the Kyoto Encyclopedia of Genes and Genomes (KEGG, as of Feb. 2009). The top reference gene(s) matching each read (bit score cutoff = 50) was used for NCBI-nr and KEGG annotations. For reads matching multiple reference genes

with equal bit score, each matching reference gene was retained as a top hit, with its representation scaled proportionately to the number of genes sharing an equal bit score. The relative transcriptional activity for a given gene was normalized to account for variations in gene abundance in the DNA pool and is presented as an expression ratio for each dataset:

$$\frac{\text{(RNA reads per gene/total RNA reads matching genes)}}{\text{(DNA reads per gene/total DNA reads matching genes)}}$$

Read counts across KEGG categories were used to cluster datasets based on shared gene content. For each sample, hit counts per KEGG category were normalized to the percentage of total reads matching the KEGG database. Pearson correlation coefficients were calculated for each pair of normalized datasets and used as similarity indices for hierarchical clustering based on the complete linkage method, as implemented in Cluster 3.0. The same analysis was repeated using read counts per unique nr taxonomic identifier as relatedness criteria, with the number of unique taxonomic identifiers per dataset standardized across datasets (mean = 1885 taxa; stdev = 0.3%).

Nucleotide sequence data generated in this study are available in the NCBI Sequence Read Archive under accession number SRA023632.1.

ACKNOWLEDGMENTS

This work was supported by a gift from the Agouron Institute. We thank Sara Lincoln, J. Francisco Santibañez, Gadiel Alarcón, and the captain and crew of the *Vidal Gormaz* for their help in collecting samples for this study, Jay McCarren for help with sample collection, DNA extractions, and metagenomic analysis, and Rachel Barry for her tireless work in preparing samples for pyrosequencing, Additional support for this work came from the Gordon and Betty

Moore Foundation (EFD), a gift from the Agouron Institute (EFD), and the Chilean Fondap Program (OU). This work is a contribution of the Center for Microbial Oceanography:

695 Research and Education (C-MORE).

References

Andrade, S.L.A., and Einsle, O. (2007) The Amt/Mep/Rh family of ammonium transport proteins. *Molecular Membrane Biology* **24**: 357-365.

700 Canfield, D.E., Stewart, F.J., Thamdrup, B., De Brabandere, L., Dalsgaard, T., DeLong, E.F., Revsbech, N.P., Ulloa, O. (2010) A cryptic sulfur cycle in oxygen-minimum-zone waters off the Chilean coast. *Science*. *In press*.

705 Carlson, C.A., Morris, R., Parsons, R., Treusch, A.H., Giovannoni, S.J., and Vergin, K. (2009) Seasonal dynamics of SAR11 populations in the euphotic and mesopelagic zones of the northwestern Sargasso Sea. *ISME Journal* **3**: 283-295.

710 Castro-Gonzalez, M., Braker, G., Farias, L., and Ulloa, O. (2005) Communities of nirS-type denitrifiers in the water column of the oxygen minimum zone in the eastern South Pacific. *Environmental Microbiology* **7**: 1298-1306.

Church, M.J., Wai, B., Karl, D.M., and DeLong, E.F. (2010) Abundances of crenarchaeal amoA genes and transcripts in the Pacific Ocean. *Environmental Microbiology* **12**: 679-688.

715 Codispoti, L.A., Brandes, J.A., Christensen, J.P., Devol, A.H., Naqvi, S.W.A., Paerl, H.W., and Yoshinari, T. (2001) The oceanic fixed nitrogen and nitrous oxide budgets: Moving targets as we enter the anthropocene? *Scientia Marina* **65**: 85-105.

720 Daneri, G., Dellarossa, V., Quinones, R., Jacob, B., Montero, P., and Ulloa, O. (2000) Primary production and community respiration in the Humboldt Current System off Chile and associated oceanic areas. *Marine Ecology-Progress Series* **197**: 41-49.

725 DeLong, E.F., Preston, C.M., Mincer, T., Rich, V., Hallam, S.J., Frigaard, N.U. et al. (2006) Community genomics among stratified microbial assemblages in the ocean's interior. *Science* **311**: 496-503.

Dhillon, A., Goswami, S., Riley, M., Teske, A., and Sogin, M. (2005) Domain evolution and functional diversification of sulfite reductases. *Astrobiology* **5**: 18-29.

730 Erguder, T.H., Boon, N., Wittebolle, L., Marzorati, M., and Verstraete, W. (2009) Environmental factors shaping the ecological niches of ammonia-oxidizing archaea. *FEMS Microbiology Reviews* **33**: 855-869.

735 Farias, L., Paulmier, A., and Gallegos, M. (2007) Nitrous oxide and N-nutrient cycling in the oxygen minimum zone off northern Chile. *Deep-Sea Research Part I-Oceanographic Research Papers* **54**: 164-180.

740 Farias, L., Castro-Gonzalez, M., Cornejo, M., Charpentier, J., Faundez, J., Boontanon, N., and Yoshida, N. (2009) Denitrification and nitrous oxide cycling within the upper oxycline of the eastern tropical South Pacific oxygen minimum zone. *Limnology and Oceanography* **54**: 132-144.

- 745 Frias-Lopez, J., Shi, Y., Tyson, G.W., Coleman, M.L., Schuster, S.C., Chisholm, S.W., and DeLong, E.F. (2008) Microbial community gene expression in ocean surface waters. *Proceedings of the National Academy of Sciences of the United States of America* **105**: 3805-3810.
- 750 Fuchs, B.M., Woebken, D., Zubkov, M.V., Burkill, P., and Amann, R. (2005) Molecular identification of picoplankton populations in contrasting waters of the Arabian Sea. *Aquatic Microbial Ecology* **39**: 145-157.
- 755 Galan, A., Molina, V., Thamdrup, B., Woebken, D., Lavik, G., Kuypers, M.M.M., and Ulloa, O. (2009) Anammox bacteria and the anaerobic oxidation of ammonium in the oxygen minimum zone off northern Chile. *Deep-Sea Research Part II-Topical Studies in Oceanography* **56**: 1125-1135.
- Gomez-Alvarez, V., Teal, T.K., and Schmidt, T.M. (2009) Systematic artifacts in metagenomes from complex microbial communities. *The ISME Journal* **3**: 1314-1317.
- 760 Hallam, S.J., Mincer, T.J., Schleper, C., Preston, C.M., Roberts, K., Richardson, P.M., and DeLong, E.F. (2006a) Pathways of carbon assimilation and ammonia oxidation suggested by environmental genomic analyses of marine Crenarchaeota. *Plos Biology* **4**: 520-536.
- 765 Hallam, S.J., Konstantinidis, K.T., Putnam, N., Schleper, C., Watanabe, Y., Sugahara, J. et al. (2006b) Genomic analysis of the uncultivated marine crenarchaeote Cenarchaeum symbiosum. *Proceedings of the National Academy of Sciences of the United States of America* **103**: 18296-18301.
- 770 Hamersley, M.R., Lavik, G., Woebken, D., Rattray, J.E., Lam, P., Hopmans, E.C. et al. (2007) Anaerobic ammonium oxidation in the Peruvian oxygen minimum zone. *Limnology and Oceanography* **52**: 923-933.
- 775 Hewson, I., Poretsky, R.S., Tripp, H.J., Montoya, J.P., and Zehr, J.P. (2010) Spatial patterns and light-driven variation of microbial population gene expression in surface waters of the oligotrophic open ocean. *Environmental Microbiology* **12**: 1940-1956.
- 780 Hewson, I., Poretsky, R.S., Beinart, R.A., White, A.E., Shi, T., Bench, S.R. et al. (2009) In situ transcriptomic analysis of the globally important keystone N₂-fixing taxon *Crocospaera watsonii*. *The ISME Journal* **3**: 618-631.
- Jayakumar, A., O'Mullan, G.D., Naqvi, S.W.A., and Ward, B.B. (2009) Denitrifying Bacterial Community Composition Changes Associated with Stages of Denitrification in Oxygen Minimum Zones. *Microbial Ecology* **58**: 350-362.
- 785 Jensen, M.M., Petersen, J., Dalsgaard, T., Thamdrup, B. (2009) Pathways, rates, and regulation of N₂ production in the chemocline on an anoxic basin, Mariager Fjord, Denmark. *Marine Chemistry* **113**: 102-113.
- 790 Jetten, M.S.M., van Niftrik, L., Strous, M., Kartal, B., Keltjens, J.T., and Op den Camp, H.J.M. (2009) Biochemistry and molecular biology of anammox bacteria. *Critical Reviews in Biochemistry and Molecular Biology* **44**: 65-84.
- 795 Kartal, B., Kuypers, M.M.M., Lavik, G., Schalk, J., den Camp, H.J.M.O., Jetten, M.S.M., and Strous, M. (2007a) Anammox bacteria disguised as denitrifiers: nitrate reduction to dinitrogen gas via nitrite and ammonium. *Environmental Microbiology* **9**: 635-642.

- 800 Kartal, B., van Niftrik, L., Rattray, J., de Vossenberg, J.L.C.M.V., Schmid, M.C., Damste, J.S.S. et al. (2008) Candidatus 'Brocadia fulgida': an autofluorescent anaerobic ammonium oxidizing bacterium. *Fems Microbiology Ecology* **63**: 46-55.
- Kartal, B., Rattray, J., van Niftrik, L.A., van de Vossenberg, J., Schmid, M.C., Webb, R.I. et al. (2007b) Candidatus "Anammoxoglobus propionicus" a new propionate oxidizing species of anaerobic ammonium oxidizing bacteria. *Systematic and Applied Microbiology* **30**: 39-49.
- 805 Konneke, M., Bernhard, A.E., de la Torre, J.R., Walker, C.B., Waterbury, J.B., and Stahl, D.A. (2005) Isolation of an autotrophic ammonia-oxidizing marine archaeon. *Nature* **437**: 543-546.
- 810 Konstantinidis, K.T., Braff, J., Karl, D.M., and DeLong, E.F. (2009) Comparative Metagenomic Analysis of a Microbial Community Residing at a Depth of 4,000 Meters at Station ALOHA in the North Pacific Subtropical Gyre. *Applied and Environmental Microbiology* **75**: 5345-5355.
- Kuenen, J.G. (2008) Anammox bacteria: from discovery to application. *Nature Reviews Microbiology* **6**: 320-326.
- 815 Kuwahara, H., Yoshida, T., Takaki, Y., Shimamura, S., Nishi, S., Harada, M. et al. (2007) Reduced genome of the thioautotrophic intracellular symbiont in a deep-sea clam, *Calyptogena okutanii*. *Current Biology* **17**: 881-886.
- 820 Kuypers, M.M.M., Lavik, G., Woebken, D., Schmid, M., Fuchs, B.M., Amann, R. et al. (2005) Massive nitrogen loss from the Benguela upwelling system through anaerobic ammonium oxidation. *Proceedings of the National Academy of Sciences of the United States of America* **102**: 6478-6483.
- 825 Kuypers, M.M.M., Sliemers, A.O., Lavik, G., Schmid, M., Jorgensen, B.B., Kuenen, J.G. et al. (2003) Anaerobic ammonium oxidation by anammox bacteria in the Black Sea. *Nature* **422**: 608-611.
- 830 Labrenz, M., Sintes, E., Toetzke, F., Zumsteg, A., Herndl, G.J., Seidler, M., and Jürgens, K. (2010) Relevance of a crenarchaeotal subcluster related to Candidatus Nitrosopumilus maritimus to ammonia oxidation in the suboxic zone of the central Baltic Sea. *The ISME Journal*.
- 835 Lam, P., Jensen, M.M., Lavik, G., McGinnis, D.F., Muller, B., Schubert, C.J. et al. (2007) Linking crenarchaeal and bacterial nitrification to anammox in the Black Sea. *Proceedings of the National Academy of Sciences of the United States of America* **104**: 7104-7109.
- Lam, P., Lavik, G., Jensen, M.M., van de Vossenberg, J., Schmid, M., Woebken, D. et al. (2009) Revising the nitrogen cycle in the Peruvian oxygen minimum zone. *Proceedings of the National Academy of Sciences of the United States of America* **106**: 4752-4757.
- 840 Lavik, G., Stuhmann, T., Bruchert, V., Van der Plas, A., Mohrholz, V., Lam, P. et al. (2009) Detoxification of sulphidic African shelf waters by blooming chemolithotrophs. *Nature* **457**: 581-586.
- 845 Leigh, J.A., and Dodsworth, J.A. (2007) Nitrogen regulation in bacteria and archaea. *Annual Review of Microbiology* **61**: 349-377.
- Li, W.Z., and Godzik, A. (2006) Cd-hit: a fast program for clustering and comparing large sets of protein or nucleotide sequences. *Bioinformatics* **22**: 1658-1659.

- 850 Martens-Habbena, W., Berube, P.M., Urakawa, H., de la Torre, J.R., and Stahl, D.A. (2009) Ammonia oxidation kinetics determine niche separation of nitrifying Archaea and Bacteria. *Nature* **461**: 976-U234.
- 855 McCarren, J., Becker, J.W., Repeta, D.J., Shi, Y.M., Young, C.R., Malmstrom, R.R. et al. (2010) Microbial community transcriptomes reveal microbes and metabolic pathways associated with dissolved organic matter turnover in the sea. *Proceedings of the National Academy of Sciences of the United States of America* **107**: 16420-16427.
- 860 Meyer, B., and Kuever, J. (2007a) Molecular analysis of the diversity of sulfate-reducing and sulfur-oxidizing prokaryotes in the environment, using *aprA* as functional marker gene. *Applied and Environmental Microbiology* **73**: 7664-7679.
- 865 Meyer, B., and Kuever, J. (2007b) Phylogeny of the alpha and beta subunits of the dissimilatory adenosine-5'-phosphosulfate (APS) reductase from sulfate-reducing prokaryotes - origin and evolution of the dissimilatory sulfate-reduction pathway. *Microbiology-Sgm* **153**: 2026-2044.
- 870 Molina, V., and Farias, L. (2009) Aerobic ammonium oxidation in the oxycline and oxygen minimum zone of the eastern tropical South Pacific off northern Chile (similar to 20 degrees S). *Deep-Sea Research Part II-Topical Studies in Oceanography* **56**: 1009-1018.
- 875 Molina, V., Belmar, L., and Ulloa, O. (2010) High diversity of ammonia-oxidizing archaea in permanent and seasonal oxygen-deficient waters of the eastern South Pacific. *Environmental Microbiology*.
- 880 Molina, V., Ulloa, O., Farias, L., Urrutia, H., Ramirez, S., Junier, P., and Witzel, K.P. (2007) Ammonia-oxidizing beta-Proteobacteria from the oxygen minimum zone off northern Chile. *Applied and Environmental Microbiology* **73**: 3547-3555.
- 885 Newton, I.L.G., Woyke, T., Auchtung, T.A., Dilly, G.F., Dutton, R.J., Fisher, M.C. et al. (2007) The *Calyptogena magnifica* chemoautotrophic symbiont genome. *Science* **315**: 998-1000.
- 890 Poretsky, R.S., Sun, S.L., Mou, X.Z., and Moran, M.A. (2010) Transporter genes expressed by coastal bacterioplankton in response to dissolved organic carbon. *Environmental Microbiology* **12**: 616-627.
- 895 Poretsky, R.S., Hewson, I., Sun, S.L., Allen, A.E., Zehr, J.P., and Moran, M.A. (2009) Comparative day/night metatranscriptomic analysis of microbial communities in the North Pacific subtropical gyre. *Environmental Microbiology* **11**: 1358-1375.
- 900 Preston, C.M., Wu, K.Y., Molinski, T.F., and DeLong, E.F. (1996) A psychrophilic crenarchaeon inhabits a marine sponge: *Cenarchaeum symbiosum* gen nov, sp, nov. *Proceedings of the National Academy of Sciences of the United States of America* **93**: 6241-6246.
- Prosser, J.I., and Nicol, G.W. (2008) Relative contributions of archaea and bacteria to aerobic ammonia oxidation in the environment. *Environmental Microbiology* **10**: 2931-2941.

- Revsbech, N.P., Larsen, L.H., Gundersen, J., Dalsgaard, T., Ulloa, O., and Thamdrup, B. (2009) Determination of ultra-low oxygen concentrations in oxygen minimum zones by the STOX sensor. *Limnology and Oceanography-Methods* **7**: 371-381.
- 905 Schleper, C., Jurgens, G., and Jonuscheit, M. (2005) Genomic studies of uncultivated archaea. *Nature Reviews Microbiology* **3**: 479-488.
- Schmidt, I., Look, C., Bock, E., and Jetten, M.S.M. (2004) Ammonium and hydroxylamine uptake and accumulation in *Nitrosomonas*. *Microbiology-Sgm* **150**: 1405-1412.
- 910 Shi, Y.M., Tyson, G.W., and DeLong, E.F. (2009) Metatranscriptomics reveals unique microbial small RNAs in the ocean's water column. *Nature* **459**: 266-U154.
- Snel, B., Bork, P., and Huynen, M.A. (1999) Genome phylogeny based on gene content. *Nature Genetics* **21**: 108-110.
- 915 Sowell, S.M., Wilhelm, L.J., Norbeck, A.D., Lipton, M.S., Nicora, C.D., Barofsky, D.F. et al. (2009) Transport functions dominate the SAR11 metaproteome at low-nutrient extremes in the Sargasso Sea. *Isme Journal* **3**: 93-105.
- 920 Stevens, H., and Ulloa, O. (2008) Bacterial diversity in the oxygen minimum zone of the eastern tropical South Pacific. *Environmental Microbiology* **10**: 1244-1259.
- Stewart, F.J., Ottesen, E.A., and DeLong, E.F. (2010) Development and quantitative analyses of a universal rRNA-subtraction protocol for microbial metatranscriptomics. *The ISME Journal* **4**: 896-907.
- 925 Strous, M., Pelletier, E., Mangenot, S., Rattei, T., Lehner, A., Taylor, M.W. et al. (2006) Deciphering the evolution and metabolism of an anammox bacterium from a community genome. *Nature* **440**: 790-794.
- 930 Taniguchi, Y., Choi, P.J., Li, G.W., Chen, H.Y., Babu, M., Hearn, J. et al. (2010) Quantifying E-coli Proteome and Transcriptome with Single-Molecule Sensitivity in Single Cells. *Science* **329**: 533-538.
- 935 Thamdrup, B., Dalsgaard, T., Jensen, M.M., Ulloa, O., Farias, L., and Escibano, R. (2006) Anaerobic ammonium oxidation in the oxygen-deficient waters off northern Chile. *Limnology and Oceanography* **51**: 2145-2156.
- 940 Ulloa, O., and Pantoja, S. (2009) The oxygen minimum zone of the eastern South Pacific. *Deep-Sea Research Part II-Topical Studies in Oceanography* **56**: 987-991.
- Urich, T., Lanzen, A., Qi, J., Huson, D.H., Schleper, C., and Schuster, S.C. (2008) Simultaneous Assessment of Soil Microbial Community Structure and Function through Analysis of the Meta-Transcriptome. *Plos One* **3**: -.
- 945 Walker, C.B., de la Torre, J.R., Klotz, M.G., Urakawa, H., Pinel, N., Arp, D.J. et al. (2010) *Nitrosopumilus maritimus* genome reveals unique mechanisms for nitrification and autotrophy in globally distributed marine crenarchaea. *Proceedings of the National Academy of Sciences of the United States of America* **107**: 8818-8823.
- 950

- Walsh, D.A., Zaikova, E., Howes, C.G., Song, Y.C., Wright, J.J., Tringe, S.G. et al. (2009)
Metagenome of a Versatile Chemolithoautotroph from Expanding Oceanic Dead Zones. *Science*
955 **326**: 578-582.
- Ward, B.B., Devol, A.H., Rich, J.J., Chang, B.X., Bulow, S.E., Naik, H. et al. (2009)
Denitrification as the dominant nitrogen loss process in the Arabian Sea. *Nature* **461**: 78-U77.
- Weidinger, K., Neuhauser, B., Gilch, S., Ludewig, U., Meyer, O., and Schmidt, I. (2007)
960 Functional and physiological evidence for a Rhesus-type ammonia transporter in *Nitrosomonas*
europaea. *Fems Microbiology Letters* **273**: 260-267.
- Woebken, D., Lam, P., Kuypers, M.M.M., Naqvi, S.W.A., Kartal, B., Strous, M. et al. (2008) A
965 microdiversity study of anammox bacteria reveals a novel *Candidatus Scalindua* phylotype in
marine oxygen minimum zones. *Environmental Microbiology* **10**: 3106-3119.
- Wuchter, C., Abbas, B., Coolen, M.J.L., Herfort, L., van Bleijswijk, J., Timmers, P. et al. (2006)
970 Archaeal nitrification in the ocean. *Proceedings of the National Academy of Sciences of the*
United States of America **103**: 12317-12322.
- Zaikova, E., Walsh, D.A., Stilwell, C.P., Mohn, W.W., Tortell, P.D., and Hallam, S.J. (2010)
Microbial community dynamics in a seasonally anoxic fjord: Saanich Inlet, British Columbia.
Environmental Microbiology **12**: 172-191.
- 975

Table 1. Read numbers and statistics.

	DNA				RNA			
	50 m	85 m	110 m	200 m	50 m	85 m	110 m	200 m
total reads	393,403	595,662	403,227	516,426	379,333	184,386	557,762	441,273
mean length (bp)	257	253	244	250	183	206	163	161
mean GC%	38.1	38.2	40.2	41.2	49.2	50.3	47.2	49.6
rRNA reads ¹	1781	1887	1114	1355	230,593	108,059	204,922	198,584
mean length (bp)	261	262	249	265	195	221	186	191
mean GC%	48.0	46.7	47.8	46.3	52.2	51.7	51.8	51.7
non-rRNA reads ²	340,117	567,772	380,057	485,044	117,760	69,200	268,093	149,699
mean length (bp)	256	253	243	249	168	190	165	168
mean GC%	37.7	38.0	39.9	41.1	43.5	47.6	43.5	46.5
nr reads ³	204,953	341,350	215,217	274,463	42,327	16,960	81,492	39,218
unique nr refs ⁴	125,121	177,856	127,767	139,262	32,819	12,567	49,540	30,096
mean reads per ref ⁵	1.6	1.9	1.7	2.0	1.3	1.3	1.6	1.3
unique nr taxa ⁶	4028	4696	4043	4053	3183	1994	3465	2838
mean reads per taxa ⁷	51	73	53	68	13	9	24	14
KEGG reads ⁸	216,497	329,570	211,024	273,709	38,409	15,430	71,847	33,779

¹ reads matching (bit score > 50) SSU or LSU rRNA sequences via BLASTN

980 ² non-rRNA reads; duplicate reads (reads sharing 100% nucleotide identity and length) excluded

³ reads matching (bit score > 50) protein-coding genes in the NCBI-nr database (as of Nov. 26, 2009)

⁴ unique NCBI-nr references (accession numbers) identified as top BLASTX hits with bit scores > 50; for reads with multiple top hits of the same bit score, all top hit references are included

⁵ nr reads/unique nr refs

985 ⁶ unique NCBI-nr taxonomic identifiers of top BLASTX hits; ~0.6-1.0% of unique nr references contained no taxonomic identification

⁷ nr reads/unique nr rtaxa

⁸ reads matching (bit score > 50) genes in the KEGG database (as of Feb. 2009)

990

Table 2. Protein-coding gene diversity and evenness¹.

	DNA		RNA	
	<i>1/D</i>	<i>E</i>	<i>1/D</i>	<i>E</i>
50 m	10707	0.694	689	0.049
85 m	9427	0.634	70	0.006
110 m	12191	0.767	258	0.020
200 m	8413	0.575	2008	0.152

995 ¹ values are calculated for subsets of randomly selected protein-coding sequencing reads, standardized to 15,000 reads per DNA/RNA sample

1/D = Simpson's diversity, where $D = \sum P_i^2$, and P_i is the proportion of the total number of protein-coding sequences represented by the *i*th unique sequence (accession number)

E = evenness = $(1/D)/S$, where *S* is the total number of unique sequences per sample; range = 0 to 1, where 1 implies uniform equal counts per unique reference sequence

1000

1000 **Figure Legends**

Fig. 1. Relatedness of OMZ DNA and RNA datasets. Heat maps show the relative distribution of protein-coding reads matching gene categories at three levels of the KEGG hierarchy (see Figures S6-8 for KEGG gene categories) and across NCBI-nr taxonomic identifiers. Gray =
1005 missing data; white = low values, red = high values. Dendrograms are based on hierarchical clustering of Pearson correlation coefficients for each pairwise dataset comparison, with blue and red branches highlighting DNA and RNA datasets, respectively.

Fig. 2. Expression ratios (RNA/DNA) averaged across all protein-coding genes (NCBI-nr
1010 annotations) per depth. “All data” shows values uncorrected for variation in sample size. “Standardized” values are calculated for subsets of each full dataset standardized to a common size (n = 15,000 protein-coding reads each). Error bars are 95% confidence intervals.

Fig. 3. Community and expression shifts with depth in the OMZ. The fifteen most abundant taxa
1015 per depth are identified based on the NCBI taxonomic affiliation of protein-coding genes matching (top blast hit) DNA and RNA sequence reads. Percentages (%ID) adjacent to taxon names are the mean amino similarities between reads and genes within each taxon, based only on the high-scoring segment pair (HSP) in each statistically significant BLAST alignment. Similarities were averaged per gene, and then across all genes per taxon.

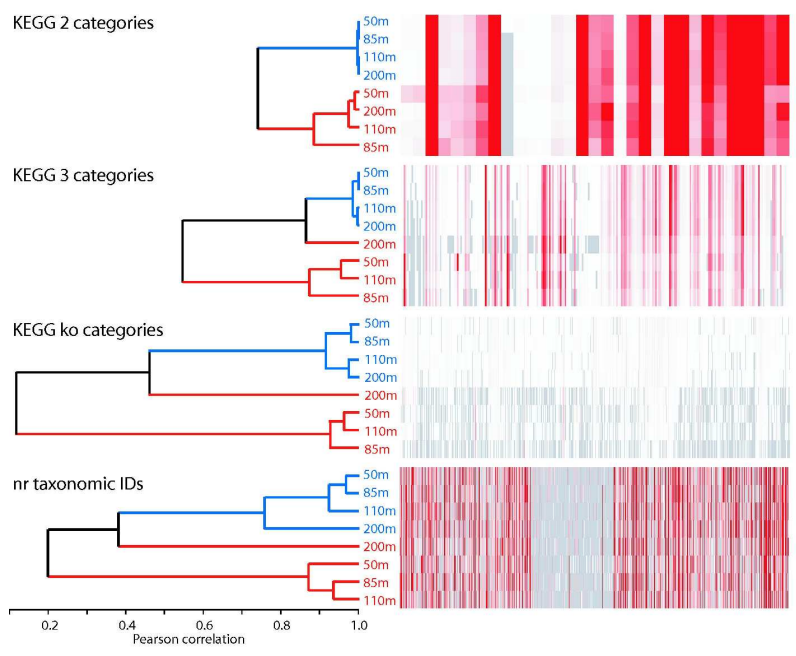
1020

Fig. 4. Relationship between DNA and RNA abundance for dominant OMZ taxa, as identified by the NCBI taxonomic affiliation of protein-coding genes matching sequence reads (as top BLASTX hit in searches against the nr database). Abundances are expressed as percentages of

the total number of reads with matches in nr (per dataset); plots show only the 100 most
1025 abundant taxa per depth (based on rankings in the RNA). Axis units are log-scaled.

Fig. 5. Distribution and abundances of DNA (blue) and RNA (red) reads with top hits to protein-coding genes in the genomes (or metagenomes) of prominent OMZ taxa: *Nitrosopumilus maritimus* (crenarchaeote, ammonia oxidizer), *Pelagibacter* sp. HTCC7211 (alpha
1030 proteobacterium, heterotroph), *Kuenenia stuttgartiensis* (planctomycete, anammox), and the SUP05 lineage (gamma proteobacteria, sulfur oxidizer). Data are shown for the depth at which each taxon was best represented, based on the proportion of genes recovered as top hits in the RNA data (Fig. 3). The total number of protein-coding genes, the mean amino acid sequence similarity of reads matching those genes (ID; mean per gene, averaged across all genes), and the
1035 mean expression ratio of genes present in both the DNA and RNA are shown below. Genes are sorted vertically by genome position (*Nitrosopumilus*, *Pelagibacter*) or accession number (*Kuenenia*, SUP05; synteny is therefore not implied for these taxa), with gene abundance (reads per gene as a percentage of total reads matching NCBI-nr genes) normalized per kb of gene length. The most abundant expressed genes and the most highly expressed genes (exp. ratio) per
1040 taxon are listed in Table S3 and S4.

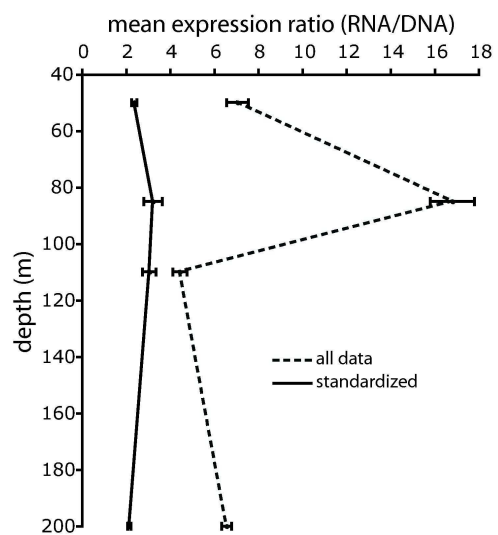
Figure 1



151x171mm (600 x 600 DPI)

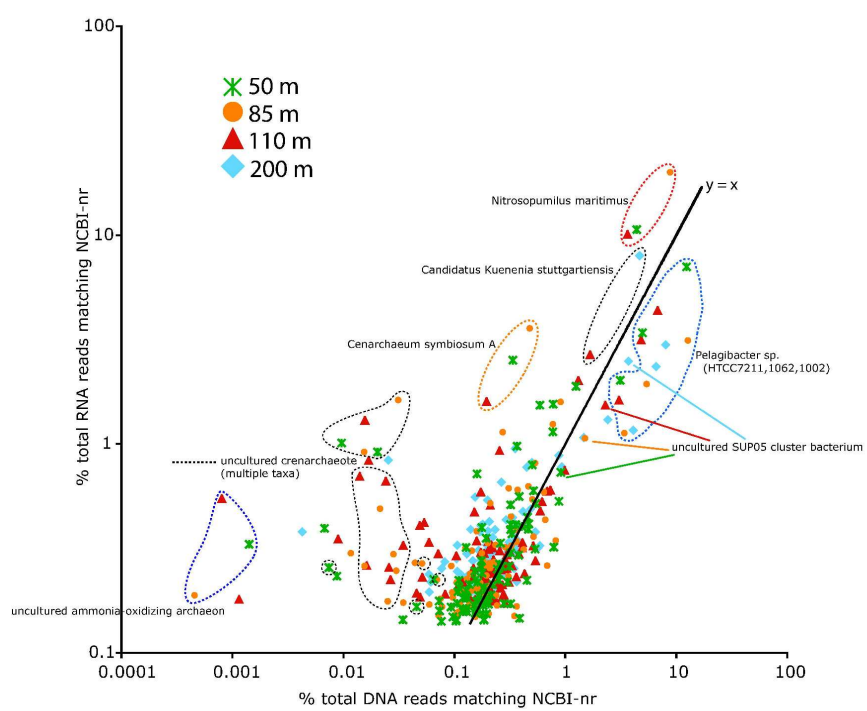


Figure 2



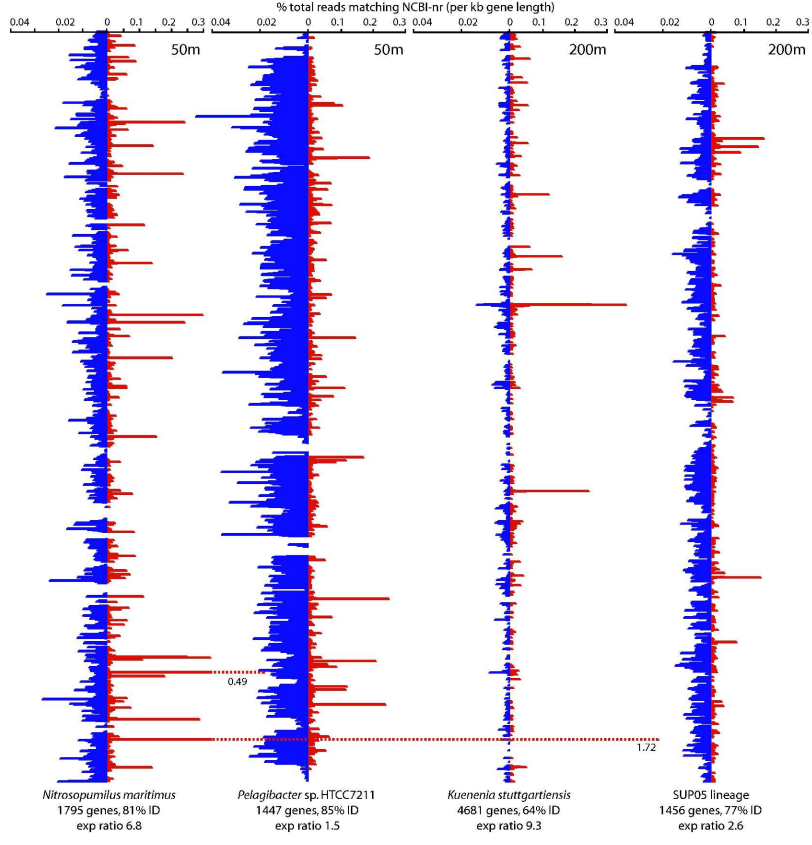
118x154mm (600 x 600 DPI)

Figure 4



150x204mm (600 x 600 DPI)

Figure 5



159x211mm (600 x 600 DPI)